Closed-loop critical curves in simple hard-sphere van der Waals-fluid models consistent with the packing fraction limit

Leonid V. Yelash,[a] Thomas Kraska,[b] and Ulrich K. Deiters
Institut für Physikalische Chemie, Universität zu Köln, Luxemburger Str. 116, D-50939 Köln, Germany

(Received 6 July 1998; accepted 5 November 1998)

Two new hard-sphere equations are proposed which, in combination with a van der Waals attraction term, lead to a biquadratic, respectively a cubic, equation of state. The new equations show the correct limiting behavior at low as well as at high densities; their poles are close to the physical packing fraction of hard spheres. Both equations of state were extended towards mixtures by one-fluid mixing rules, and their global phase behavior was investigated for the special case of equal-sized molecules. Both equations are able to predict closed-loop liquid–liquid immiscibility; the topology of the phenomenenon is the same as for the Carnahan–Starling equation. It appears the occurrence of closed-loop liquid–liquid immiscibility does not depend on the location of the pole nor on the degree of the equation of state used. © *1999 American Institute of Physics.* [S0021-9606(99)51606-1]

I. INTRODUCTION

Because closed-loop liquid–liquid immiscibility has been experimentally detected in strongly polar mixtures only, it has been attributed to hydrogen bonding for many years. Thus the early work of Boshkov,[1] who first demonstrated that this phenomenon could be obtained with an equation of state for the nonpolar Lennard-Jones fluid, was met with doubt. Meanwhile the phenomenon could be found for other equations of state for nonpolar fluids, such as the simplified perturbed hard chain equation[2] or the Redlich–Kwong[3] equation. In a recent publication[4] we have shown that the attractive hard sphere fluid, modeled by the Carnahan–Starling van der Waals equation of state[5,6] (CSvdW) is able to produce closed-loop liquid–liquid immiscibility, too.

In contrast to this, the van der Waals equation (vdW) is known to show no closed-loop liquid–liquid immiscibility. The reason for this qualitatively different behavior is still not completely understood. It has been suggested that the location of the poles of the equations of state might be responsible for the difference, and—since the CSvdW equation has its pole at too high densities—that therefore the closed-loop immiscibility obtained with this equation might be an artifact.

Another reason for the qualitative differences between the vdW and the CSvdW equation might be the cubic nature of the former as opposed to the quintic nature of the latter.

In this article we investigate the qualitative and quantitative dependence of the closed-loop phenomenon on the location of the pole and on the degree of the equation of state. We intend to give an answer to the question if the pole of the CS equation at $y_{\text{pole}}=1$ with $y\equiv(\pi/6)\sigma^3(N/V)$ is the reason for the existence of closed loops in the CSvdW model and how the closed-loop behavior changes, when the correct packing fraction limit is included in the model.

II. THEORY

The CS equation is an accurate equation of state for the hard-sphere fluid, but since it had been developed in the low density limit it does not incorporate the correct high density limit. In Fig. 1 the dependence of the the compressibility factor $Z=pV_{\text{m}}/RT$ on the packing fraction is shown for the van der Waals repulsion (vdWR) $Z_{\text{vdwR}}=1/(1-4y)$ and the CS equation $Z_{\text{CS}}=(1+y+y^2-y^3)/(1-y)^3$. The largest possible packing fraction should be 0.74 [close packing face-centered-cubic (fcc) lattice] or slightly less (random close packing). But evidently the vdW equation yields a too low maximal packing fraction ($y_{\text{pole}}=0.25$), whereas the maximal packing fraction of the CS equation is too high ($y_{\text{pole}}=1$).[7] The value of the packing fraction at the pole is determined by the values of the coefficients B_m of the virial expansion of Z

$$Z=1+\sum_{m=1}^{\infty} B_{m+1}y^m. \tag{1}$$

In Table I the virial coefficients of the van der Waals repulsion term (vdWR) and the CS equation are compared with the results obtained by a Monte Carlo (MC) integration by Ree and Hoover.[8,9] The virial coefficients of the vdWR equation ($B_i^{\text{vdWR}}=4^{i-1}$) increase too strongly with i, thus causing a too low y_{pole} value. The virial coefficients of the CS equation [$B_i^{\text{CS}}=3(i-1)+(i-1)^2$] are in good agreement with the Monte Carlo results up to B_7, but the higher virial coefficients do not increase strongly enough in order to place the pole at the correct close packing value. Generally the packing fraction at the pole of a hard sphere equation is related to the limiting behavior of the virial coefficients by the expression (see the Appendix)

[a]Permanent address: Thermodynamics Center, Academy of Refrigeration, 1/3 Dvoryanskaya Str., 270026 Odessa, Ukraine.
[b]Author to whom correspondence should be addressed; electronic mail: kraska@stthd0.pc.uni-koeln.de

 © 1999 American Institute of Physics

Downloaded 23 Jan 2003 to 134.95.49.170. Redistribution subject to AIP license or copyright, see http://ojps.aip.org/jcpo/jcpcr.jsp

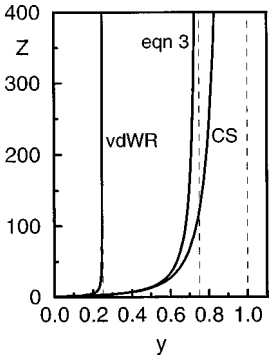

FIG. 1. Compressibility factor Z as function of the packing fraction y for the vdWR equation, the CS equation, and Eq. (3). The pole for each equation is indicated by a dashed line.

$$\lim_{m\to\infty}\left(\frac{B_m}{B_{m+1}}\right)=y_{\text{pole}}. \tag{2}$$

Equation (2) can be understood as a guideline for the construction of the higher virial coefficients, which cannot be obtained by numerical integration. One can distinguish two types of repulsion terms depending on the behavior of B_m/B_{m+1} as function of m: For vdWR-like equations B_m/B_{m+1} is constant and always equal to $y_{\text{pole}}=1/4$, for CS-like equations, B_m/B_{m+1} is a nonlinear function of m, and it is necessary to compute the limit for infinite m in order to obtain $y_{\text{pole}}=1$.

A. Modification of the CS equation

We have introduced the nearly correct pole packing fraction at 3/4 by multiplying the CS equation with $(3-4y)/(3-4y)$ and shifting the value of the coefficient of the y^4 term in the resulting equation from 4.0 to 6.0. As result we obtained the following equation for the hard sphere fluid:

$$Z=\frac{3+5y+6y^2}{(1-y)(3-4y)}. \tag{3}$$

The pole of this equation is at $y=0.75$, which is very close to the value of the close packing fraction. Comparison of Eq. (3) with simulation results of the hard sphere fluid show good agreement. The virial coefficients $[B_i=27/2\times(4/3)^{i-1}-14]$ listed in Table I are close to the CS values and the MC values up to approximately $i=5$. Higher virial coefficients of Eq. (3) increase stronger than the CS values.

TABLE I. Comparison of the repulsive virial coefficients of the van der Waals equation (vdWR), the Carnahan–Starling equation (CS), Monte Carlo results of Ree and Hoover (Refs. 8, 9) (MO), and Eqs. (3) and (7).

	Virial coefficient B_i				
i	vdW	CS	MC	Eq. (3)	Eq. (7) with $f_{\text{pole}}=4/3$
2	4	4	4	4	4
3	16	10	10	10	10
4	64	18	18.36	18	13.33
5	256	28	28.24 ± 0.08	28.67	17.78
6	1024	40	39.52 ± 0.53	42.89	23.70
7	4096	54	56.52 ± 1.64	61.85	31.60
8	16384	70	[80.28, 95.03]	87.14	42.14

The equation of state employed here for the calculation of phase equilibria consists of Eq. (3) and the van der Waals mean field attraction term

$$p=\frac{RT}{V_{\text{m}}}\left[\frac{3+5y+6y^2}{(1-y)(3-4y)}\right]-\frac{a}{V_{\text{m}}^2}. \tag{4}$$

In this equation of state the packing fraction is related to the covolume parameter b by $y=b/4V_{\text{m}}$. If we define reduced variables

$$\tilde{T}=\frac{8Rb}{a}T,\quad \tilde{p}=\frac{8b^2}{a}p, \tag{5}$$

the critical properties can be expressed as $y_{\text{c}}=0.130\,082\,08$, $\tilde{T}_{\text{c}}=3.0163\,361\,4$, $\tilde{p}_{\text{c}}=0.563\,927\,977\,5$, $Z_{\text{c}}=0.359\,307\,63$. These values can be used for the calculation of the equation of state parameters a and b from the critical temperature T_{c} and critical volume $V_{\text{m,c}}$ of a substance. The values of the reduced critical values of Eq. (4) are very close to those of the CSvdW equation of state ($y_{\text{c}}=0.130\,443\,884$, $\tilde{T}_{\text{c}}=3.018\,518\,50$, $\tilde{p}_{\text{c}}=0.565\,352\,121\,1$, $Z_{\text{c}}=0.358\,956\,21$). This is not surprising, since the differences between the CSvdW equation and Eq. (4) are important at packing fractions much higher than the critical packing fraction only.

Rearranging Eq. (4) leads to a fourth order polynomial in the molar volume,

$$24pV_{\text{m}}^4-(14bp+24RT)V_{\text{m}}^3+(2b^2p-10bRT+24a)\times V_{\text{m}}^2-(3b^2RT+14ba)V_{\text{m}}+2ab^2=0, \tag{6}$$

which is one order higher than the cubic van der Waals equation and one order lower than the fifth order Carnahan–Starling–van der Waals equation. It is therefore possible to calculate the molar volume from the pressure with Eq. (4) analytically.[10]

B. Modification of the vdWR equation

The derivation of Eq. (3) is based on the CS equation. It is also possible to start from the vdWR equation and extend it with respect to the correct close packing fraction. We have derived an equation which is designed to fulfill the following requirements:

(a) the second virial coefficient is always $B_2=4$;
(b) the pole is at $y_{\text{pole}}=1/f_{\text{pole}}$;
(c) for $f_{\text{pole}}=4$ ($y_{\text{pole}}=0.25$) the equation degenerates to the vdWR equation;
(d) for $f_{\text{pole}}=4/3$ ($y_{\text{pole}}=0.75$) the third virial coefficient is exact at $B_3=10$.

The parameter f_{pole} can be used to move the pole of the vdWR equation towards the physical limit of close packing and to decrease the value of the third virial coefficient.

$$Z=\frac{1+(4-f_{\text{pole}})y+7\left(1-\dfrac{f_{\text{pole}}}{4}\right)y^2}{1-f_{\text{pole}}y}. \tag{7}$$

Downloaded 23 Jan 2003 to 134.95.49.170. Redistribution subject to AIP license or copyright, see http://ojps.aip.org/jcpo/jcpcr.jsp

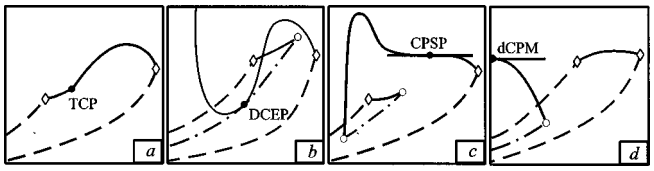

FIG. 2. Boundary states in binary phase diagrams. The dashed lines are the vapor pressure curves of the pure substances: (a) degenerated critical pressure maximum (dCPM); (b) critical pressure step point (CPSP); (c) double critical end point (DCEP); and (d) tricritical point (TCP).

The virial coefficients of this equation are $B_i=(7+9/4f_{\text{pole}})f_{\text{pole}}^{i-3}$ for $i\geqslant 3$. They are listed in Table I for $f_{\text{pole}}=4/3$. This family of equations is of vdWR type in two respects:

(a) if combined with the vdW attraction it yields a cubic equation of state in the molar volume;
(b) it has constant values for B_m/B_{m+1}.

Inserting $f_{\text{pole}}=4/3$ into Eq. (7) and combining it with the van der Waals attraction yields the equation of state

$$p=\frac{RT}{V_{\text{m}}}\left(\frac{3+8y+14y^2}{3-4y}\right)-\frac{a}{V_{\text{m}}^2}. \tag{8}$$

Equation (8) can be rearranged to its cubic form

$$-3pV_{\text{m}}^3+(3RT+pb)V_{\text{m}}^2+(2RTb-3a)V_{\text{m}}+ab+\tfrac{7}{8}RTb^2=0. \tag{9}$$

The critical properties of Eq. (8) are $y_{\text{c}}=0.138\,692\,40$, $\tilde{T}_{\text{c}}=3.091\,635\,97$, $\tilde{p}_{\text{c}}=0.609\,271\,360\,9$, and $Z_{\text{c}}=0.355\,230\,10$. As Eq. (6), Eq. (9) can be solved analytically.

C. Extension to mixtures

For the investigation of the binary phase behavior Eqs. (4) and (8) have been extended by usual quadratic mixing rules. Since we focus here on equal sized spheres only, we have $b=b_{11}=b_{22}=b_{12}$ and

$$a=\sum_{i=1}^{2}\sum_{j=1}^{2}x_i x_j a_{ij}. \tag{10}$$

The method of the investigation of the phase behavior of binary mixtures employed here has been introduced by van Konynenburg and Scott.[11,12] It has been further developed recently in many articles.[13–16] The axes of a global phase diagram are reduced differences of the equation of state parameters

$$\lambda=\frac{d_{22}-2d_{12}+d_{11}}{d_{22}+d_{11}}, \tag{11}$$

$$\zeta=\frac{d_{22}-d_{11}}{d_{22}+d_{11}}. \tag{12}$$

Here $d_{ij}=T_{ij}^{*}b_{ij}/b_{ii}b_{jj}$ is the interaction density and $T_{ij}^{*}=a_{ij}/Rb_{ij}$ the characteristic temperature. For equal sized spheres the d_{ij} can be replaced by a_{ij} in the definitions of the global parameters λ and ζ. The regions of the global phase diagram represent different types of binary phase behavior.

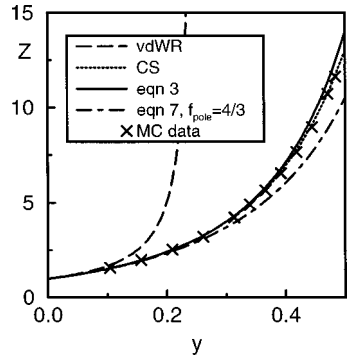

FIG. 3. Comparison of the compressibility factor obtained with the vdWR equation, the CS equation, Eq. (3), Eq. (7), and Monte Carlo results of Barker and Henderson (Ref. 17).

These regions are separated by boundary lines which are higher order thermodynamic states and can be calculated by numerically solving the corresponding analytically available thermodynamic conditions. For a detailed discussion of the boundary states related to the closed-loop behavior see Ref. 4. In Fig. 2 the boundary states related to the appearance of the closed-loop liquid–liquid immiscibility are shown in the corresponding $p-T$ projection of the binary phase diagrams.

III. RESULTS

A. Hard-sphere fluid

Figure 3 shows a comparison of the compressibility factor of Eq. (3) with Z_{CS} and results obtained by Monte Carlo simulation by Barker and Henderson.[17] The comparison of the pair correlation function at contact corresponding to Eq. (3)

$$g(\sigma)=\frac{3+y/2}{(1-y)(3-4y)} \tag{13}$$

and Eq. (7)

$$g(\sigma)=\frac{1+(\frac{7}{4}-\frac{7}{16}f_{\text{pole}})y}{1-f_{\text{pole}}y}, \tag{14}$$

and from Monte Carlo simulation data is shown in Fig. 4. Both comparisons show that Eq. (3) is in very good agreement with the simulation data up to $y\simeq 0.4$. For higher y Eq. (3) gives slightly larger values than the simulation and the

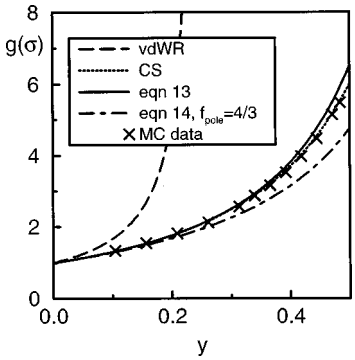

FIG. 4. Comparison of the pair correlation function at contact obtained with Eq. (3), Eq. (7), and Monte Carlo results of Barker and Henderson (Ref. 17).

Downloaded 23 Jan 2003 to 134.95.49.170. Redistribution subject to AIP license or copyright, see http://ojps.aip.org/jcpo/jcpcr.jsp

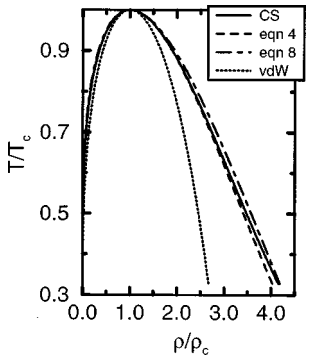

FIG. 5. Comparison of the coexistence curve of a pure substance obtained with the CS equation, Eq. (4), and Eq. (8) with $f_{\text{pole}}=4/3$.

CS term. But since Eq. (3) includes the high density limit very close to the close packing value the values of Eq. (3) and the simulation data are expected to approach each other at higher packing fraction. This of course neglects the glassy state found at $y\simeq 0.6$,[18] as all fluid equations of state neglect solid phases.

Equation (7) shows larger deviations from the MC data than Eq. (3), but it is still a reasonable model for the hard sphere fluid. For any value of f_{pole} it is certainly a better approximation than the vdWR equation. The inferior agreement of its virial coefficients with the exact values is due to the simplification of the equation structure to a cubic equation of state [Eq. (7)].

B. Phase equilibria of pure fluids

Figure 5 shows a temperature density plot of the coexistence curve for the CSvdW equation in comparison with the biquadratic Eq. (4), the cubic Eq. (8), and the vdW equation. Obviously the differences in the saturated liquid densities between Eqs. (4), (8), and CSvdW are small. Equation (4) shows a slight decrease of the liquid density as compared to the CSvdW model. The saturated liquid densities calculated with Eq. (8) at $T/T_c>0.3$ are slightly larger than CSvdW liquid densities. Both new equations show a very good agreement of the saturated vapor densities with those of the CSvdW equation.

C. Phase equilibria of mixtures

In order to investigate the influence of the different repulsions terms on the binary phase behavior we have calculated the global phase diagrams for the biquadratic and the cubic equations and compared it with the global phase diagram obtained with the CSvdW equation.[4] Sections of the global phase diagrams showing all important regions of binary phase diagrams, are plotted in Fig. 6. The $p-T$ diagrams corresponding to the boundary curves plotted in Fig. 6 are shown in Fig. (2). The closed-loop region obtained with the CSvdW equation[4] [Fig. 6 (top)] is surrounded by the two branches of the critical pressure step point line [CPSP, Fig. 2(b)], one branch of the double critical end point line [DCEP, Fig. 2(c)], and the degenerated critical pressure maximum line [dCPM, Fig. 2(a)]. At the CPSP line the binary phase diagram type V forms two additional extremes

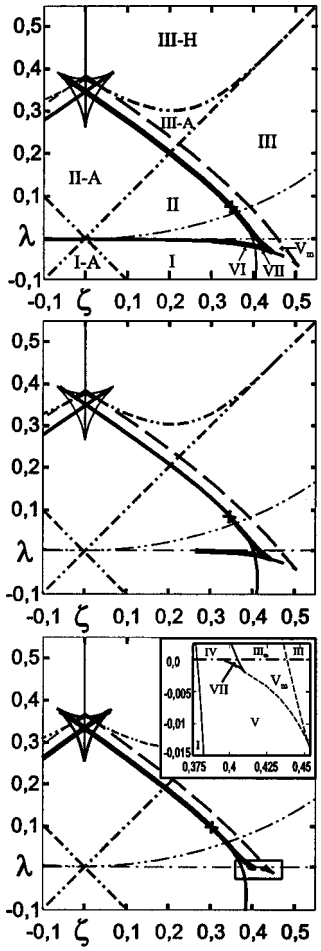

FIG. 6. Global phase diagram calculated with different equations of state. Top: CS equation; middle: Eq. (4); bottom with magnification of the closed-loop region: Eq. (8). (—) DCEP, (—) TCP, (– – –) CPSP, (---) dCPM, (---) azeotrope boundary lines, (---) geometric mean line ($a_{12}=\sqrt{a_{11}a_{22}}$), (+) van Laar point.

and changes to type V_{m}. At the dCPM the liquid–liquid critical line changes its slope and direction at $T=0$ K and therefore produces an extreme in the liquid–liquid critical line. The triangle-like closed-loop region is divided into three parts by two more boundary lines. At the DCEP line [Figure 2(c)] a binary critical line touches the three-phase line and type V_{m} changes to type VII. At the tricritical line [TCP, Fig. 2(d)] the three-phase line interrupting the liquid gas critical line shrinks to a point, and type VII changes to type VI.

Most parts of the global phase diagrams are very similar for all three equations. The region which is most sensitive to the changes in the the repulsive virial coefficients is the closed-loop region. Figure 6 show the closed-loop regions for the biquadratic and the cubic equation of state. The closed-loop behavior obtained with the biquadratic equation is topologically identical to the behavior obtained with the CSvdW equation.[4] These two equations differ only in the absolute position and size of the closed-loop region. They both produce the binary phase diagram types V_{m}, VII, and VI as described above. The closed loop region obtained with the cubic equation differs in one point topologically from the one obtained with the CSvdW equation: The short branch of

Downloaded 23 Jan 2003 to 134.95.49.170. Redistribution subject to AIP license or copyright, see http://ojps.aip.org/jcpo/jcpcr.jsp

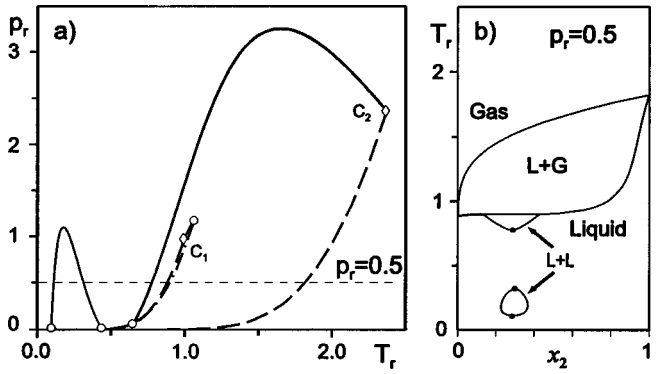

FIG. 7. A binary phase diagram type VII calculated with Eq. (8) ($\zeta = 0.4065$, $\lambda = -0.0008$: (a) pT-projection; (b) one xT_r-section at $p_r = 0.5$; $T_r = T/T_{c,1}$; $p_r = p/p_{c,1}$.

the DCEP line, starting at the DCEP cusp, ends near the dCPM line for numerical reasons. Since this numerically caused end point is very close to the dCPM line and far from the TCP line, the existence of the binary phase diagram type VI is unlikely. Hence the cubic equation produces the closed-loop types V_m and VII but not VI. Type VII has an isolated closed-loop island as type VI. Figure 7 shows a phase diagram of type VII calculated with the cubic equation.

IV. CONCLUSIONS

In this article two equations of state have been developed which reproduce the physical properties of the hard-sphere fluid well and have simple mathematical structures. In contrast to the CS equation they both have a pole close to the physically correct close-packing fraction and reproduce the virial coefficients much better than the vdWR equation. Similar equations can be found in the literature[19–23] of which some are slightly better, but always at the cost of a more complicated equation structure. The equations proposed here yield biquadratic and cubic equations in V_m when combined with a vdW-kind attraction. Therefore $V_m = V_m(p,T)$ can be solved analytically, which makes them attractive for applications.

The calculation of the pure substance liquid–gas coexistence curves shows very good agreement with the CSvdW equation. The analysis of the binary mixture behavior shows that the unphysically high packing fraction at the pole of the CS term is not the reason for the closed-loop behavior of the CSvdW equation of state: An equation of state with the nearly correct packing fraction limit produces the same closed-loop behavior as the CSvdW equation. Parts of the closed-loop critical lines may correspond to metastable states in real mixtures, e.g., they are below the crystallization planes, but they are not at unphysically high packing fraction beyond the fcc close packing fraction. This investigation confirms the existence of closed-loop liquid–liquid critical lines in the attractive hard-sphere fluid mixtures.

We have shown that the existence of the closed-loop behavior does not depend on the order of the equation of state. It is possible to obtain closed loops with the quintic CSvdW equation as well as with the the quartic Eq. (4) or the cubic Eq. (8). It appears that the important properties are the values of the repulsive virial coefficients. If they are close to the hard-sphere values, one can expect closed-loop behavior after combination with the vdW attraction term. As shown above, the value of y_{pole} is related to the values of the higher virial coefficients by Eq. (2). However the y_{pole} value also affects the values of the lower virial coefficients. For a simple vdWR-type equation $Z = 1/(1-fy)$ the strong correlation between B_i and y_{pole} $[B_i = (1/y_{pole})^{i+1}]$ becomes obvious for all virial coefficients. It follows that with decreasing y_{pole} towards the unphysically low vdWR value of 0.25 the virial coefficients get unphysically large. Along this path towards the vdWR equation the closed-loop behavior vanishes. Hence the pole of this simple equation has an indirect influence on the existence of closed loops, equations of state with the physically correct pole and repulsive virial coefficients of the hard-sphere fluid clearly do exhibit closed-loop behavior.

ACKNOWLEDGMENTS

This study was supported by the Deutsche Forschungsgemeinschaft (DFG) and the Fonds der Chemischen Industrie. One of the authors (T.K.) has received a Habilitandenstipendium of the DFG.

APPENDIX

Derivation of Eq. (2): Before considering the relations between virial coefficients we note that the geometrical series

$$S_0 = \sum_{i=0}^{\infty} q^i = \frac{1}{1-q}, \tag{A1}$$

converges for $|q| < 1$. By differentiating this equation higher order expressions can be obtained

$$S_n = \frac{\partial^n S_0}{\partial q^n} = \sum_{i=0}^{\infty} \frac{(i+n)!}{i!} q^i = \frac{n!}{(1-q)^{n+1}}. \tag{A2}$$

The factor $(i+n)!/i!$ is a polynomial in i of the order n. By forming appropriate linear combinations of the S_n it is always possible to isolate the i^n term

$$\sum_{i=0}^{\infty} i q^i = S_1 - S_0, \tag{A3}$$

$$\sum_{i=0}^{\infty} i^2 q^i = S_2 - 3S_1 + S_0, \tag{A4}$$

$$\vdots$$

generally

$$\sum_{i=0}^{\infty} i^n q^i = \sum_{k=0}^{n} p_{nk} S_k. \tag{A5}$$

Hence it is possible to express any infinite series $\Sigma i^n q^i$ by a finite series of S_n, and convergence is certain for $|q| < 1$. The virial series Eq. (1) must converge for all densities below the pole $y < y_{pole}$ and diverge at $y = y_{pole}$. We assume that the virial coefficients can be expressed as finite or infinite series

Downloaded 23 Jan 2003 to 134.95.49.170. Redistribution subject to AIP license or copyright, see http://ojps.aip.org/jcpo/jcpcr.jsp

$$B_{m+1}=\sum_{i=0} b_{im}m^i. \tag{A6}$$

Inserting this into Eq. (1) leads to

$$Z=\sum_{m=0}^{\infty}\sum_{i=0} b_{im}m^i y^m=\sum_{i=0}\sum_{m=0}^{\infty}(b_{im}y^m)m^i. \tag{A7}$$

The expression in parentheses is identified with q^m, i.e., we assume

$$q=(-1)^{1-\mathrm{sgn}(b_{im})}b_{im}^{1/m}y, \tag{A8}$$

where sgn represents the sign function. Then we can rewrite (A7) as

$$Z=\sum_{i=0}\sum_{k=0}^{i} p_{ik}\frac{i!}{(1-q)^{i+1}}. \tag{A9}$$

In order to ensure convergence at all densities $0\leqslant y<y_{\mathrm{pole},i}$, $|q|<1$ must hold. At the pole we have $|q|=1$ for all m above some finite threshold. Hence

$$|b_{im}|=\frac{1}{y_{\mathrm{pole},i}^m} \tag{A10}$$

and

$$B_{m+1}=\sum_{i=0}\frac{m^i}{y_{\mathrm{pole},i}^m}. \tag{A11}$$

Equation (A6) diverges if at least one of the inner sums diverges. Let i' denote the index whose series diverges first. Then the virial expansion converges for $0\leqslant y<y_{\mathrm{pole}}$ with

$$y_{\mathrm{pole}}=y_{\mathrm{pole},i'}\leqslant y_{\mathrm{pole},i\neq i'}. \tag{A12}$$

For large values of m the contribution of i' to Eq. (A12) therefore dominates

$$\lim_{m\to\infty} B_{m+1}=\frac{m^{i'}}{y_{\mathrm{pole}}^m} \tag{A13}$$

and finally

$$\lim_{m\to\infty}\frac{B_m}{B_{m+1}}=y_{\mathrm{pole}}. \tag{A14}$$

[1] L. Z. Boshkov, Dokl. Akad. Nauk SSSR **294**, 901 (1987).
[2] A. van Pelt, C. J. Peters, and J. de Swaan Arons, J. Chem. Phys. **95**, 7569 (1991).
[3] L. Z. Boshkov and L. V. Yelash, Dokl. Akad. Nauk SSSR **340**, 622 (1995).
[4] L. V. Yelash and T. Kraska, Ber. Bunsenges. Phys. Chem. **102**, 213 (1998).
[5] J. D. van der Waals, in *Studies in Statistical Mechanics*, edited by J. S. Rowlinson (North-Holland, Amsterdam, 1988), Vol. XIV.
[6] N. F. Carnahan and K. E. Starling, J. Chem. Phys. **51**, 635 (1969); AIChE. J. **18**, 1184 (1972).
[7] In practical calculations, the size parameter σ is adjusted to give an acceptable description of the liquid phase behavior. But this can only be achieved at the expense of the correct behavior at low densities.
[8] F. H. Ree and W. G. Hoover, J. Chem. Phys. **40**, 939 (1964).
[9] F. H. Ree and W. G. Hoover, J. Chem. Phys. **46**, 4181 (1967).
[10] J. E. Hacke, Am. Math. Monthly **48**, 327 (1941); FORTRAN and *C* code available at http://www.uni-koeln.de/math-nat-fak/phchem/deiters/quartic/quartic.html.
[11] R. L. Scott and P. H. van Konynenburg, Discuss. Faraday Soc. **49**, 87 (1970).
[12] P. H. van Konynenburg and R. L. Scott, Philos. Trans. R. Soc. London, Ser. A **298A**, 495 (1980).
[13] U. K. Deiters and I. L. Pegg, J. Chem. Phys. **90**, 6632 (1989).
[14] T. Kraska and U. K. Deiters, J. Chem. Phys. **96**, 539 (1992).
[15] L. Z. Boshkov, Ber. Bunsenges. Phys. Chem. **96**, 910 (1992).
[16] L. Z. Boshkov and L. V. Yelash, Fluid Phase Equilibria **141**, 105 (1997).
[17] J. A. Barker and D. Henderson, Mol. Phys. **21**, 187 (1971).
[18] L. V. Woodcook, Ann. (N.Y.) Acad. Sci. **371**, 274 (1981).
[19] B. Baeyens and H. Verschelde, J. Math. Phys. **36**, 201 (1995).
[20] M. J. Maeso, J. R. Solana, J. Amoros, and E. Villar, J. Chem. Phys. **94**, 551 (1991).
[21] J. I. Goldman and J. A. White, J. Chem. Phys. **89**, 6403 (1988).
[22] Y. Song, R. M. Stratt, and E. A. Mason, J. Chem. Phys. **88**, 1126 (1988).
[23] M. K. Khoskbarchi and J. H. Vera, Fluid Phase Equilibria **130**, 189 (1997).

Downloaded 23 Jan 2003 to 134.95.49.170. Redistribution subject to AIP license or copyright, see http://ojps.aip.org/jcpo/jcpcr.jsp